ELSEVIER

Chemical Engineering Journal 108 (2005) 203–212

Chemical Engineering Journal

www.elsevier.com/locate/cej

Experimental investigation and particle dynamic simulation for synthesizing titania nanoparticles using diffusion flame

Ruoyu Hong [a,b,*], Zhiqiang Ren [a], Jianmin Ding [c], Hongzhong Li [b]

[a] *Department of Chem. Eng. and Key Lab. of Organic Synthesis of Jiangsu Prov., Soochow University, 1 Shi Zhi St., Suzhou 215006, China*
[b] *Key Lab. of Multiphase Reaction, Institute of Process Engineering, Chinese Academy of Sciences, Beijing 100080, China*
[c] *IBM, HYDA/050-3 C202, 3605 Highway 52 North, Rochester, MN 55901, USA*

Received 15 October 2004; received in revised form 29 January 2005; accepted 1 February 2005

Abstract

Using titanium tetrachloride ($TiCl_4$) as a precursor, titania (TiO_2) nanoparticles were synthesized in the diffusion flame (DF) of air and liquid petrol gas (LPG). The effects of air and LPG flow rates and flow ratio, flame temperature and flame shape on the synthesized titania nanoparticles were investigated. Experimental investigation showed that the mean particle size of TiO_2 increased obviously with increasing airflow rate, and not obviously with that of LPG, the mean particle size at optimal experimental condition was less than 20 nm, the rutile fraction in the synthesized powder increased with increasing flame temperature and the particle size was affected by the flame height. A particle-dynamic model, describing the nucleation and coagulation of titania monomers/nanoparticles, was used to account for the experimental results based on the isothermal assumption. Generally speaking, the calculated particle sizes from the particle dynamics were consist with the experimental measurements, especially, when the feed concentration of $TiCl_4$ was low.

Keywords: Combustion; Diffusion flame; Nanoparticle; Titania; Particle dynamics

1. Introduction

Titanium dioxide (or titania, chemical formula TiO_2), which is innocuous and harmless to health, is the major white pigment. Moreover, it is the most important product that contains titanium. About 90% of the titanium ores are used to produce titania.

The aqueous suspension of titania nanoparticles is capable of decomposing organic wastes under the UV irradiation [1–3]. The organic wastes, which are difficult to be disposed using traditional methods, can be easily destroyed by photo catalysis using titania nanoparticles. Therefore, many scientists are paying attention to the synthesis methods and photocatalytic properties of titania nanoparticles.

Methods for synthesizing titania nanoparicles can be classified into gas-phase synthesis and liquid-phase synthesis. For the former, the typical examples are the sol–gel method [4], the solution hydrolysis method [5] and the supercritical method [6]. For the latter, the typical examples are the gas combustion synthesis [7,8] and the plasma synthesis [9]. Difficulties and challenges remain in the above synthesis methods, e.g., severe agglomeration and mal-dispersion in the gas-phase synthesis; and high cost to be paid for using the liquid-phase synthesis. The gas combustion using diffusion flame (DF) [7,8,10] is a promising method since the size of nanoparticles can be controlled and the dispersion of nanoparticles is good. Furthermore, the diffusion flame synthesis (DFS) might be easier scale-up from laboratory to massive manufacturing facility. Therefore, researchers all over the world are paying much attention to different aspects of the DFS [11–14].

In the traditional gas-phase combustion method [7,8] for synthesizing titania nanoparticles, hydrogen (H_2) was used as the fuel, oxygen as the oxidant, and the dried argon (Ar) as the gas carrier to feed titanium tetrachloride into the high-temperature flame [11]. Prepared TiO_2 by oxidation of $TiCl_4$

* Corresponding author. Tel.: +86 512 6724 1197; fax: +86 512 6522 4783.
E-mail addresses: rhong@suda.edu.cn (R. Hong), jading@us.ibm.com (J. Ding).

1385-8947/$ – see front matter © 2005 Elsevier B.V. All rights reserved.
doi:10.1016/j.cej.2005.02.011

Nomenclature

a	mean particle surface area (m^2)
a_s	surface area of a completely fused aggregate (m^2)
C	particle velocity
C_{TiCl_4}	$TiCl_4$ concentration (mol/m^3)
D	particle diffusion coefficient
D_f	mass fractal-like dimension
d_p	primary particle diameter (m)
g	transition parameter
N	particle-number concentration (m^{-3})
P	total pressure of system (Pa)
Q	gas flow rate (m^3/s)
R	gas constant (J/mol K)
r_c	collision diameter (m)
T	temperature (K)
v	mean solid volume (m^3)
β	coagulation kernel
ρ	gas density (kg/m^3)
τ	characteristic sintering time (s)

in diffusion flames using methane (CH_4). But the cost of the product in China might be quite high since the hydrogen and methane are comparatively expensive. In the present investigation, the liquid petroleum gas (LPG) and air were used instead of hydrogen and oxygen to reduce the cost. The TiO_2 nanoparticles were synthesized and the operating conditions were varied in present experiments. The particle dynamic simulation was conducted to predict the particle size.

2. Experimental

During the synthesis of nanoparticles by DFS, it is very important to adjust the temperature, the velocity and the particle residence time in the flame to control the particle size and crystallinity. The experimental flow diagram is illustrated in Fig. 1.

The main chemicals used in the experiments are: $TiCl_4$ (chemical grade, Shanghai Chemical Works) as the precursor and liquid petroleum gas (LPG, industrial grade) as fuel. There are two gas routeways of the combustion system. For the first one, LPG flows through the drier (No. 1 in Fig. 1), and then flows through the rotameter (No. 3), and finally flows into the combustor (No. 5). For the second one, air compressed by the air compressor (No. 8), flows through the drier (No. 1′), the rotameter (No. 3′) and the evaporator (No. 2) one after another. The $TiCl_4$ vapor, carried into the diffusion flame by the dried air, is almost instantaneously converted into titania monomers via the following oxidation

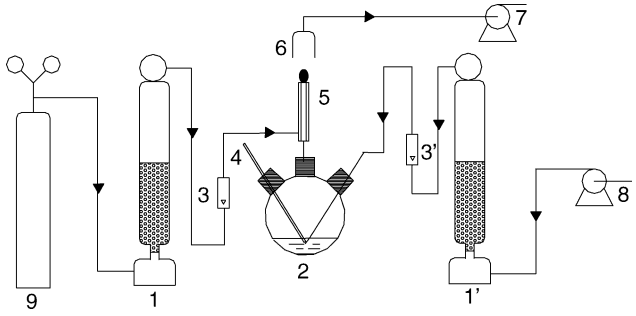

Fig. 1. Experimental flow diagram for synthesizing TiO_2 nanoparticles using LPG/air flame. (1 and 1′: Dryer, 2: $TiCl_4$ evaporator, 3 and 3′: rotameters, 4: thermometer, 5: combustor, 6: filter, 7: circulating-water vacuum pump, 8: air compressor, 9: LPG cylinder).

and hydrolysis reactions [7]:

$$TiCl_4 + 4H_2O \rightarrow Ti(OH)_4 + 4HCl,$$

$$Ti(OH)_4 \rightarrow TiO_2 + 2H_2O,$$

$$TiCl_4 + O_2 \rightarrow TiO_2 + 2Cl_2.$$

The nucleation, nuclei growth and coagulation in the vapor phase take place one after another. The high temperature stream, which mixed with entrained cold air since a vacuum pump was used in the experiment, was quenched. Therefore, nanosized titania particles were obtained.

Since a circulating-water vacuum puma was used in the experiment, the corrosive HCl was absorbed by water. The feed concentration of $TiCl_4$ vapor was calculated based on the air flow rate and the weight loss of liquid $TiCl_4$ of the evaporator. The evaporator was operated at 30 °C.

The configuration of the LPG/air combustor is illustrated in Fig. 2. The combustor used in the experiments consists of two concentric glass tubes. Inner diameters of the inner and outer tubes are 3.5 and 9.0 mm, respectively. The length of the combustor is 150 mm. The flow rates of LPG and air were varied in the experiments to investigate their effects on the particle size and crystallinity. A ceramic filter (No. 6), which was placed above the flame and was connected to a circulating-water vacuum pump, was used to capture the synthesized nanoparticles.

A transmitting electron microscope (TEM, H-600, Hitachi, Japan) was used to measure the size and shape of synthesized TiO_2 nanoparticles. The X-ray diffraction (XRD) analyzer (D/Max-IIIC, Rigaku, Japan) for powders was performed using Cu Kα radiator. The rutile content of the product can be calculated by integrating the area of the XRD peak.

3. Particle-dynamic simulation

The size using of nanoparticles can be predicted using the particle dynamic model [15,16,12].

In the present investigation we assumed that titania monomers, formed by finite oxidation reaction, grow into

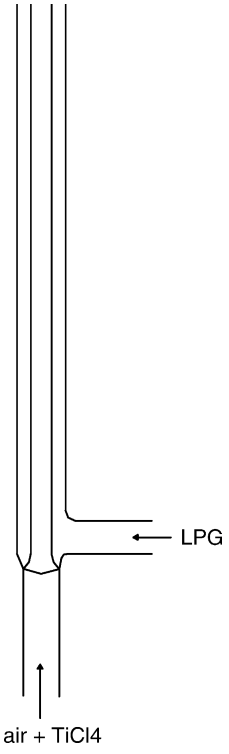

Fig. 2. Illustration of combustor configuration.

molecular clusters and small particles by successive collision, coagulation and sintering. The particle dynamic simulations based on the assumption of instantaneous reaction have been performed by [17,18].

A particle-dynamic model [19,20] was modified to describe the collision, coagulation and sintering of nanoparticles during the DFS.

The rate equation of the $TiCl_4$ oxidation can be expressed as

$$\frac{dC_{TiCl_4}}{dt} = -k_0 e^{-\frac{E_a}{RT}} C_{TiCl_4} \quad (1)$$

where E_a is the activation energy, k_0 is the pre-exponential factor and C_{TiCl4} is the $TiCl_4$ concentration. According to [21], $E_a = 88.8 \pm 3.2$ kJ/mol and $k_0 = 8.29 \times 10^4\ s^{-1}$.

Assuming all aggregates contain the same number of equally sized monomer particles, particle-number concentration can be expressed as

$$\frac{dN}{dt} = -k_0 e^{-\frac{E_a}{RT}} C_{TiCl_4} - \frac{1}{2}\beta N^2 \rho_g \quad (2)$$

The volume of an aggregate, v, is only affected by coagulation,

$$\frac{dv}{dt} = -\frac{1}{N}\frac{dN}{dt} v \quad (3)$$

The surface area of an aggregate particle, a, which increases by coagulation and decreases by sintering [22], can be described by,

$$\frac{da}{dt} = -\frac{1}{N}\frac{dN}{dt} a - \frac{1}{\tau}(a - a_s) \quad (4)$$

According to [19], the coagulation kernel β is calculated using the Eq. (5) instead of the solid sphere radius in the Fuchs interpolation [23]:

$$r_c = \left(\frac{v}{v_p}\right)^{1/D_f} r_p s \quad (5)$$

The coagulation kernel β using the Fuchs interpolation expression for Brownian coagulation in the free molecule and continuum regimes [23] takes the following form,

$$\beta = 8\pi D r_c \left[\frac{r_c}{2r_c + \sqrt{2}g} + \frac{\sqrt{2}D}{C r_c}\right]^{-1} \quad (6)$$

where the expressions of particle diffusion coefficient D, particle velocity C, and transition parameter g can be found in [19].

The characteristic sintering time, τ, is given by [24]. The mass fractal dimension, D_f, which equals three for a spherical particle and two for a circular paarticle, decreases with increasing aggregation. According to [25], a constant mass fractal dimension of $D_f = 1.8$ was used in the present simulation.

According to [20], the surface area of a completely fused aggregate is

$$a_s = \pi^{1/3}(6v)^{2/3} \quad (7)$$

The primary particle diameter [19] is

$$d_p = \frac{6v}{a} \quad (8)$$

The ordinary differential equations (Eqs. (1–4)) together with the constitutional equations (Eqs. (5–8)) are strongly coupled and nonlinear, and can only be solved numerically. The calculated primary results are the $TiCl_4$ concentration, particle-number concentration (N), mean solid volume (v), and mean particle surface area (a).

The temperature profile of the flame was not measured in the present investigation, although, such measurements were performed by [13]. Therefore, constant temperature of the flame was assumed in the numerical simulation. Similar treatment was used by [2,17,19,24,30].

4. Results and discussion

4.1. Characteristics of the flame

The flame height and temperature under different air and LPG flow rates are listed in Table 1. The flame height was obtained by naked eyes using a ruler. The flame temperature was measured using a platinum-rhodium thermocouple (type

Table 1
Flame height and temperature at different flow rates

Airflow rate (cm^3/s)	LPG flow rate (cm^3/s)	Flame height (cm)	Maximum flame temperature (°C)
66.1	0.667	2.5	620
66.1	0.833	3.0	650
66.1	1.00	3.9	677
66.1	1.17	6.0	720
66.1	1.33	7.2	780
66.1	1.67	8.2	864
66.1	2.33	8.3	880
55.6	1.17	6.0	720
50.0	1.17	4.7	686
44.4	1.17	3.2	683
38.9	1.17	3.0	690

R). It was found that the flame temperature should be sampled without the introduction of $TiCl_4$, since the generated TiO_2 was easily adhered to the surface of the thermocouple. The flame temperature with $TiCl_4$ oxidation and hydrolysis might be somehow different to the values listed in Table 1. The measured temperatures were corrected in order to take account of the heat losses by radiation.

4.2. Influence of feed mode

The inlet positions of air, LPG and $TiCl_4$ were changed during the experiments. It was found that when the mixture of air and $TiCl_4$ was fed into the inner tube, and LPG was fed into the outer tube, nanoparticles with minimum diameter were synthesized. Our experimental findings agree with the results of [26].

4.3. Influence of LPG flow rate

The variation of mean particle size and size distribution were investigated by fixing the airflow rate at 61.1 cm^3/s and increasing the flow rate of fuel (LPG) from 0.667, 0.833, 1.00, 1.17, 1.33, 1.67 to 2.33 cm^3/s in turn. Fig. 3 illustrated the influence of LPG flow rate on the mean particle diameter of synthesized titania. The minimum particle size, (d_p ~18 nm) can be obtained with air flow rate = 61.1 cm^3/s and LPG flow rate = 0.833–1.00 cm^3/s. Fig. 4 shows the TEM photographs

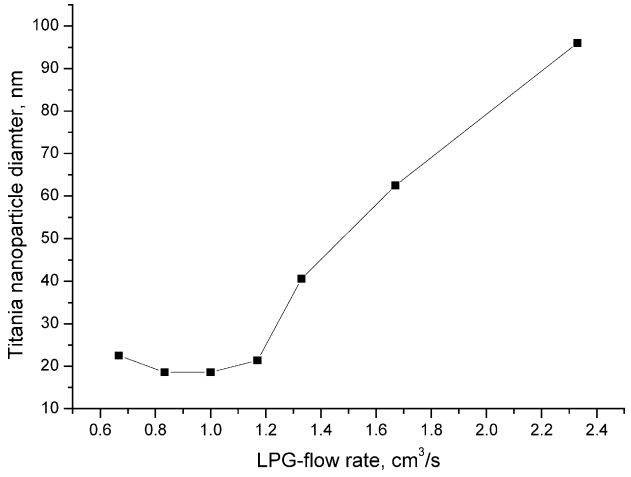

Fig. 3. Mean particle size of TiO_2 at different LPG flow rates.

of synthesized TiO_2 nanoparticles under different LPG flow rates.

When the LPG flow rate increased from 0.667, 0.833, 1.00 to 1.17 cm^3/s in turn, the flame height was not improved too much, resulting in almost the same particle sizes. When the LPG flow rate increased further, the particle sized increased too, and this trend was observed by [11].

The oxidation of $TiCl_4$ at high temperature is extraordinary fast and completes within a very short period of time [8]. When the LPG flow rate is low, the flame height and the residence time are very short. The small TiO_2 nanoparticles have too little time to coagulate and hence the particle size is small. However, if the LPG flow rate is too low, the flame temperature will also be low. This results in difficulty to maintain the flame and therefore limit titania production rate. In the present investigation, we have seen that the flame can be easily extinguished if the LPG flow rate is less than 0.667 cm^3/s.

When the LPG flow rate increases, both flame height and flame temperature increase relatively fast. The coagulation coefficient and the residence time of titania monomers/nanoparticles increase as well. Hence, the diameter of the synthesized titania nanoparticles increases rapidly.

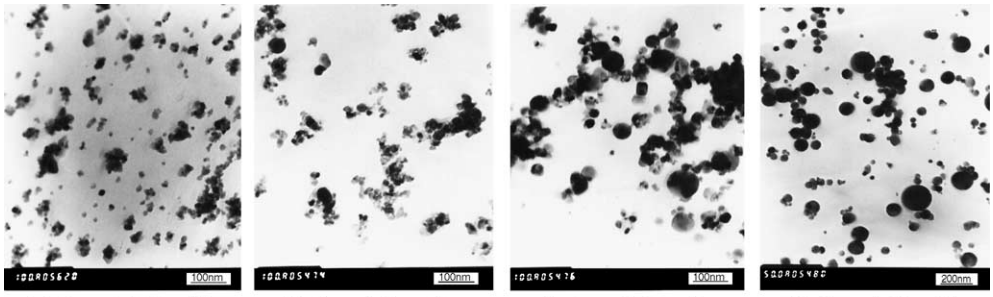

(a) Q_{LPG}=0.667 cm^3/s (b) Q_{LPG}=1.00 cm^3/s (c) Q_{LPG}=1.67 cm^3/s (d) Q_{LPG}=2.33 cm^3/s

Fig. 4. TEM photographs of TiO_2 nanoparticles synthesized at different LPG flow rates. (a) Q_{LPG} = 0.667 cm^3/s (b); Q_{LPG} = 1.00 cm^3/s; (c) Q_{LPG} = 1.67 cm^3/s; (d) Q_{LPG} = 2.33 cm^3/s.

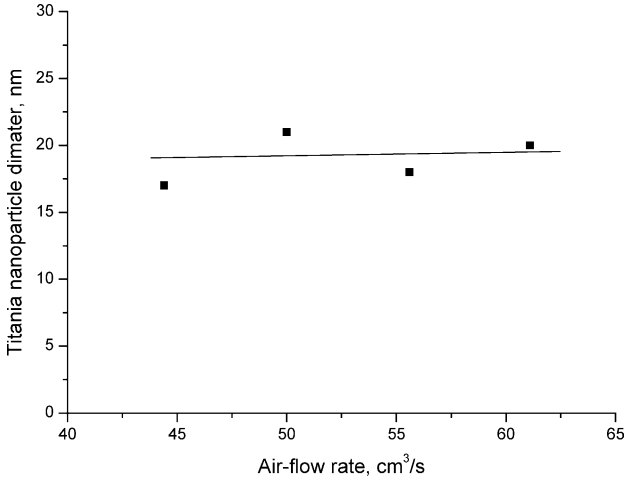

Fig. 5. Mean diameter of TiO_2 nanoparticles at different airflow rates.

When the LPG flow rate is larger than 2.33 cm^3/s, the flame color is yellow. The color of synthesized powder becomes yellowish since there are some TiO_x ($x < 2$) and carbon black in the product. Therefore, the flow rate of LPG should be kept much less than 2.33 cm^3/s, and the optimal LPG flow rate should be at 1.17 cm^3/s with the air flow rate of 61.1 cm^3/s.

4.4. Influence of air flow rate

The synthesized TiO_2 size and its distribution were investigated by fixing the LPG flow rate at 1.17 cm^3/s and decreasing air flow rate from 61.1, 55.6, 50.0 to 44.4 cm^3/s in turn. Fig. 5 illustrates the influence of airflow rate on the mean diameter of synthesized TiO_2 particles. The TEM photographs of the TiO_2 nanoparticles are shown in Fig. 6.

When the air flow rate increased, the total inlet $TiCl_4$ was increased, but the feed concentration of $TiCl_4$ was almost the same.

The mean diameter of TiO_2 nanoparticles increases slightly with the increasing airflow rate, which might be due to the two major factors: residence time and flame temperature. When the airflow rate increases, the flame temperature increases while the flame height decreases, as shown in Table 1. The particle coagulation rate increases with temperature but the particle residence time in the flame decreases with decreasing of the flame height. The two factors compete with each other and reach an equivalent, resulting in little change of particle size. To obtain higher yields, the optimal airflow rate may be kept at 61.1 ml/s.

4.5. Influence of flame temperature

Fig. 7 is the TGA of the synthesized TiO_2 nanoparticles, which were obtained at the LPG flow rate of 1.17 cm^3/s and airflow rate of 61.1 cm^3/s. The TGA tests were performed under the protection of inert gas, and the temperature rising rate was 20 °C per minute. Fig. 7 shows that there is a weight loss between 100 and 180 °C, indicating the release of physically-absorbed water. The weight loss between 180 and 750 °C is attributed to the loss of chemically bound water. Since the powder contains carbon and the titania could be deoxidized by carbon at very high temperature, there is a significant weight reduction between the temperature of 830 and 1000 °C. The results are in accordance with the findings of [14].

It can also be seen from Fig. 7 that there are two obvious peaks at the temperatures of 600 and 804 °C, respectively. The two peaks are related with the nucleation, nuclei growth and coagulation that took place in the high-temperature flame [24]. During the DFS of TiO_2 nanoparticles, the oxidation of $TiCl_4$ mainly results in the molecular clusters of anatase titania at first. Then the following rival reactions take place: the molecular clusters of anatase titania will coagulate to form anatase particles, or will transform into rutile molecular clusters. The nucleation rate is high enough to result in many anatase molecular clusters. Those molecular clusters collide

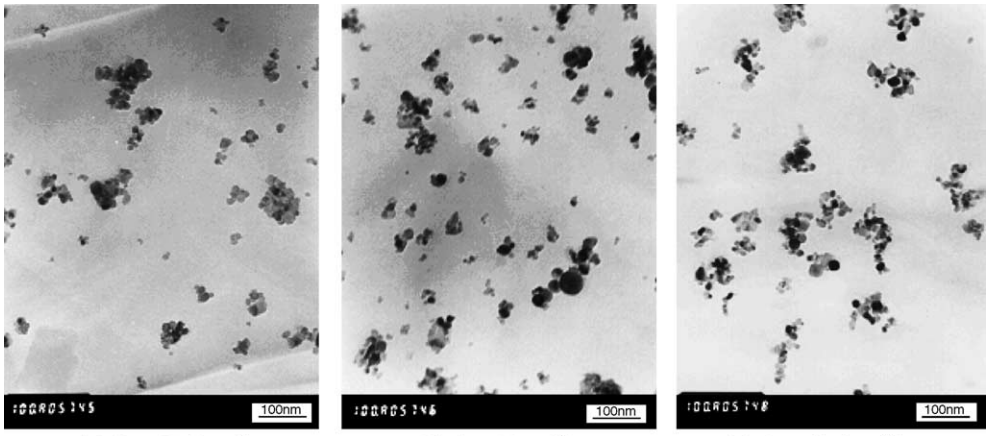

(a) Q_{air}=55.6 cm^3/s (b) Q_{air}=50 cm^3/s (c) Q_{air}=44.4 cm^3/s

Fig. 6. TEM photographs of TiO_2 nanoparticles synthesized at different airflow rates. (a) Q_{air} = 55.6 cm^3/s; (b) Q_{air} = 50 cm^3/s; (c) Q_{air} = 44.4 cm^3/s.

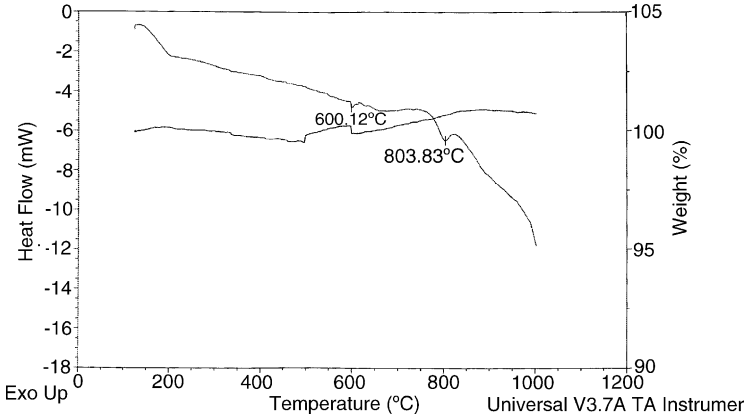

Fig. 7. TGA spectra of TiO_2 nanoparticles.

with each other to form anatase particles. Since the LPG/air flame is used instead of the H_2/air flame, the flame temperature is relatively low, many crystalline defects are generated in the produced particles [27]. Therefore, the heat-flux peak at 600 °C (see Fig. 7) is due to improvement of the anatase with eliminating crystalline defects. The heat-flux peak (see Fig. 7) at 804 °C can be attributed to the crystallinity transformation from anatase to rutile.

Fig. 8 is the XRD patterns of the titania synthesized at different flame temperatures. It can be seen that the characteristic diffraction peak of rutile (1 1 0, 2θ =27.4°) increases gradually with increasing temperature.

It could be seen from Fig. 8 that there were peaks at 2θ = 36.15047, 41.21630, 70.68966 and 75.15987. These peaks correspond to a series of characteristic peaks: 2.499(1 1 1), 2.1637(2 0 0), 1.5302(2 2 0), 1.3047(3 1 1), 1.2492(2 2 2) in the pattern of titanium carbide. The *d* values calculated from the XRD patterns were well indexed to the titanium carbide (International Center for Diffraction Data, JCPDS 32-1383), implying the presence of TiC. The average crystallite size *D* was calculated using the Debye–Scherrer formula $D = K\lambda/(\beta \cos\theta)$, where *K* is Scherrer constant, λ is the x-ray wavelength, β is the peak width of half-maximum, and θ is the Bragg diffraction angle. The crystallite size thus obtained from this equation was found to be about 10.2 nm, which is basically in accordance with the sizes from TEM images, and particle-dynamic simulation shown in Section 4.8. It could also be found in Fig. 8 that the peaks of TiC are not recognizable below 800 °C, and become significant at the temperature of 864 and 880 °C. The finding is also in accordance with the TGA analysis.

Fig. 9 illustrated the influence of flame temperature on rutile content in the synthesized titania, which was calculated by integrating the area of X-ray diffraction peak. When the flame temperature is lower than 800 °C, most of the product is the anatase (anatase content >95%). Moreover, the rutile content increases slowly with the increasing flame temperature. When the flame temperature is higher than 800 °C, the rutile content increases rapidly with flame temperature. These trends are in accordance with the TGA spectra shown in

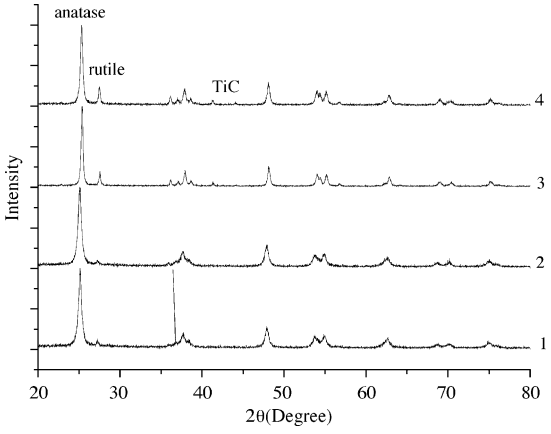

Fig. 8. X-ray diffraction patterns for TiO_2 synthesized at different flame temperatures. (1) Q_{air} = 66.1 cm^3/s, Q_{LPG} = 1.00 cm^3/s, T = 677 °C, (2) Q_{air} = 66.1 cm^3/s, Q_{LPG} = 1.33 cm^3/s, T = 780 °C, (3) Q_{air} = 66.1 cm^3/s, Q_{LPG} = 1.67 cm^3/s, T = 864 °C, (4) Q_{air} = 66.1 cm^3/s, Q_{LPG} = 2.33 cm^3/s, T = 880 °C.

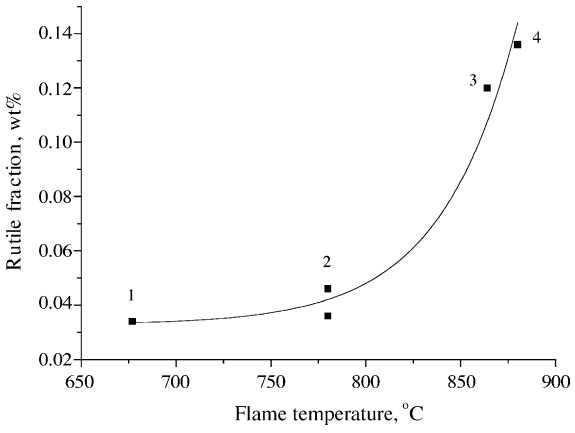

Fig. 9. Rutile content of titania nanoparticles synthesized at different flame temperatures. (1) Q_{air} = 66.1 cm^3/s, Q_{LPG} = 1.00 cm^3/s, T = 677 °C, (2) Q_{air} = 66.1 cm^3/s, Q_{LPG} = 1.33 cm^3/s, T = 780 °C, (3) Q_{air} = 66.1 cm^3/s, Q_{LPG} = 1.67 cm^3/s, T = 864 °C, (4) Q_{air} = 66.1 cm^3/s, Q_{LPG} = 2.33 cm^3/s, T = 880 °C.

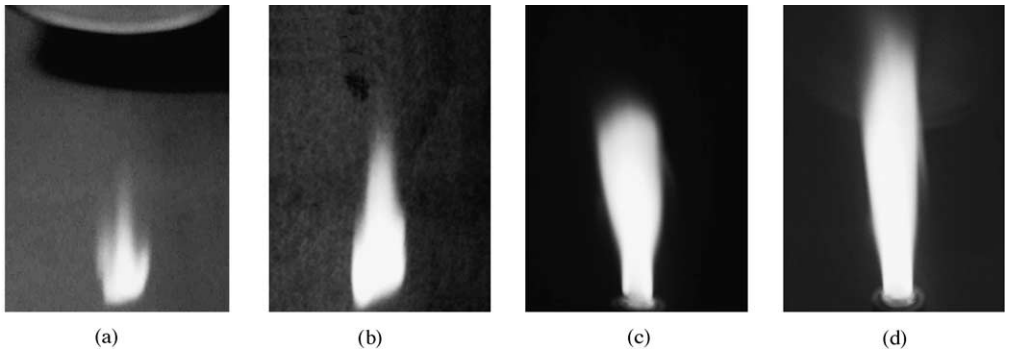

Fig. 10. Flame shapes at different LPG flow rates. (a) Q_{air} = 61.1 cm^3/s, Q_{LPG} = 0.889 cm^3/s (b) Q_{air} = 61.1 cm^3/s, Q_{LPG} = 1.11 cm^3/s (c) Q_{air} = 61.1 cm^3/s, Q_{LPG} = 1.67 cm^3/s (d) Q_{air} = 61.1 cm^3/s, Q_{LPG} = 2.33 cm^3/s.

Fig. 7. Since the flame temperature is only slightly higher than the crystallinity transformation temperature and the particle residence time in the flame is very short, most of the synthesized nanoparticles are therefore the anatase (anatase content >80%). The LPG contents mostly the butane and propane. Compared with hydrogen, the combustion rate of LPG in air is relatively slow, and the flame temperature is relatively low. Therefore, the LPG/air flame is suitable for synthesizing the anatase titania, which has high efficiency for photo-catalytic degradation of organic wastes.

4.6. Influence of flame shape

When the concentration and temperature are fixed, the diameter of titania is determined primarily by the residence time of monomers/particles in the flame. Therefore, the diameter distribution strongly depends on the residence time distribution.

Fig. 10 shows the flame shape at different LPG flow rate with air flow rate at 61.1 cm^3/s. We saw that, there is the horizontal movement of monomers/particles while moving upwards in the flame. The particle size distribution is affected by the flame height and width. When the LPG flow rate is low enough, the flame is short, the residence times for the titania monomers/particles traveling upward through in the center of flame and out of the edge of flame are almost the same. In this case, particles with smaller size could be obtained. When the LPG flow rate increases, the flame height increases rapidly, and the ratio of residence times for particles traveling upward through the center of flame to the outer edge of flame becomes larger. In this case, particles with larger size are expected. Therefore, TiO_2 nanoparticles with narrow size distribution could be obtained at low LPG flow rates.

4.7. Photo catalytic properties of TiO_2 nanoparticles

The experiments for photo-catalytic degradation of methyl orange were performed in a reactor shown in Fig. 11. The i.d. of the outer tube is 4 cm, the i.d. of the inner tube is 2 cm, and the height of the tube is 10 cm. During all the experiments, the liquid surface is in the middle of the tube and is 16 cm below the UV lamp. The power of the UV lamp is 30 W. Cooling water is flowing inside the jacket of the reactor in order to keep the photo-catalytic reaction take place under constant temperature. More details about the experimental apparatus can be found in reference [29].

The procedures for the photo-catalytic degradation are as follows: 0.3 g photo-catalyst (titania nanoparticles, synthesized under the following conditions: Q_{air} = 66.1 cm^3/s, Q_{LPG} = 1.00 cm^3/s, T = 677 °C) was put into 100 ml aqueous solution of methyl orange (5×10^{-5} mol/L). The aqueous suspension was put into the reactor (as shown in Fig. 11), and stirred by a magnetic agitator for 20 min. The photo-catalytic degradation was conducted under the UV irradiation at 25 °C. Some suspension, which was taken out of the reactor every hour, was centrifuged, and the upper lucid liquid was used to measure its UV–visible light absorption. Fig. 12 illustrates the UV–vis absorptivity at different time intervals. The numbers in Fig. 12 indicated the number of hours for photo-catalytic degradation. Compared with another photo catalyst ZnO [28,29], the photo-catalytic activity of TiO_2 synthesized in the present investigation is much higher. It may be due to the fact that the titania was doped with carbon during the DFS. The energy belt of titania was reduced, and hence the photo-catalytic activity was improved. It was also found that

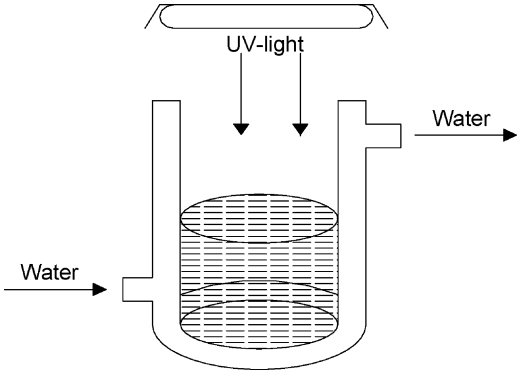

Fig. 11. Experimental apparatus for photo-catalytic degradation.

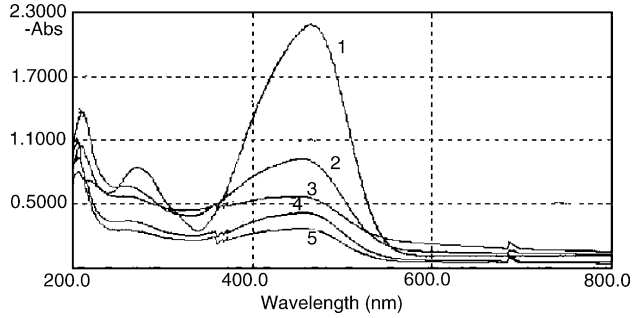

Fig. 12. UV–vis absorption of methyl orange solution sampled every hour during degradation.

the titania photo-catalyst can be used for many times without any obvious decline of photo-catalytic activity.

4.8. Predictions of titania diameter from simulations

The particle-dynamic simulation was performed at various conditions to investigate their effects on particle sizes. The titania nanoparticle diameter is plotted as a function of the axial direction. The axial direction could be explained as the flame height.

4.8.1. Particle size versus airflow rate

In the particle dynamic simulation, the reaction temperature is fixed at 1200 K and $TiCl_4$ feed concentration is at 0.005 mol/L. The variation of titania particle diameter with the airflow rate is illustrated in Fig. 13. The TiO_2 diameter increases in the flow direction through the flame. When the airflow rate increases, the TiO_2 diameter decreases since the residence time decreases.

4.8.2. Particle size versus $TiCl_4$ feed concentration

The reaction temperature is fixed at 1200 K and airflow rate at 0.20 m^3/s. The variation of titania particle diameter with the $TiCl_4$ feed concentration of is illustrated in Fig. 14. It could be found that the TiO_2 diameter increases with the increasing feed concentration, which agrees with experimental results presented in previous Section 4.3.

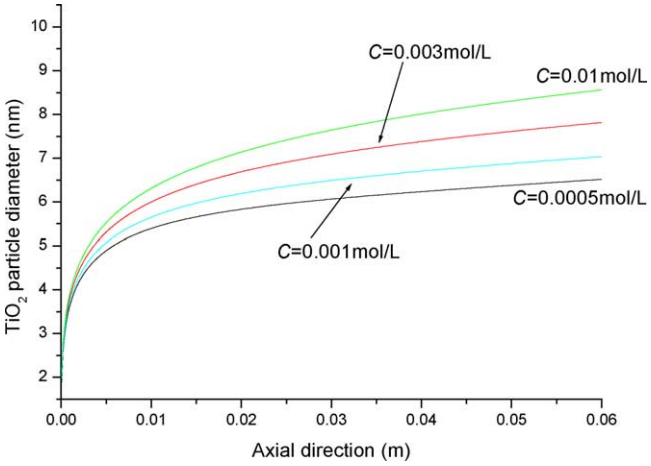

Fig. 14. Influence of $TiCl_4$ concentration on titania diameter.

4.8.3. Particle size versus reaction temperature

To investigate the influence of reaction temperature on titania diameter, the feed concentration of $TiCl_4$ is fixed at 0.005 mol/L and airflow rate at 0.20 m^3/s. The variation of titania diameter with the reaction temperature is illustrated in Fig. 15. It shows that the TiO_2 diameter increases significantly with the reaction temperature.

4.9. Simulated versus measured particle sizes

By comparing the simulated results (Figs. 13–15) with the measured data (Figs. 3 and 5), it can be found that the difference between the simulated and measured particle sizes is not large when the feed concentration of $TiCl_4$ is relatively low. The general trends are similar: the size of titania nanoparticles increases with the increasing reaction temperature and the increasing $TiCl_4$ concentrations. When the reaction temperature is fixed, the particle size decreases with

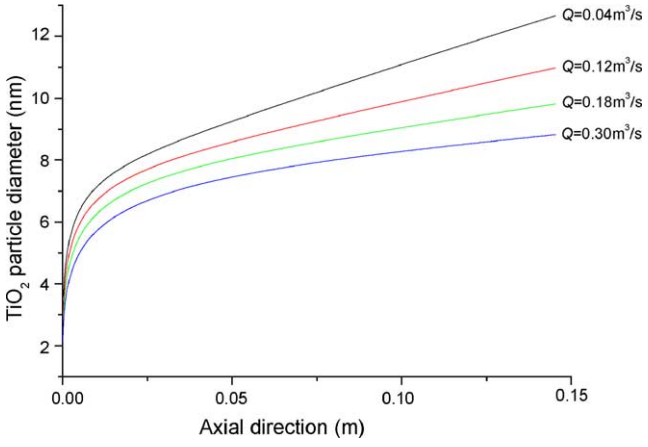

Fig. 13. Influence of airflow rate on titania diameter.

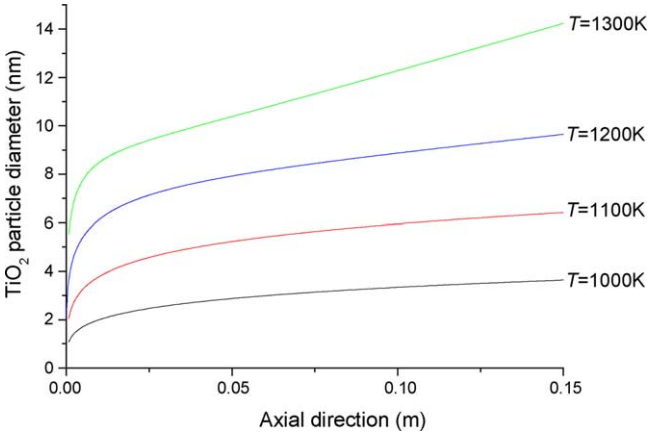

Fig. 15. Influence of reaction temperature on titania diameter.

the increasing air flow rates. During the experiments, when the LPG flow rate increases, the reaction temperature and flame length increase at the same time, leading to the larger particle size. Thus, the particle size increases obviously with LPG flow rate in the experiments. On the other hand, when we increase the air flow rate, we also increase the LPG flow rate in general. Therefore, the reaction temperature increases and the residence time decreases. The two trends of reaction temperature and flow rate counteract, resulting in almost the same particle size.

The differences between the simulated results and the measured data are relatively large at high feed concentrations. Relatively larger TiO_2 particles can be seen in the TEM photographs (see Figs. 4 and 6). This might be due to the following reasons: (1) the fixed temperatures used in the numerical simulations are different to actual situations in which the temperatures are varied with wide distributions in the diffusion flame. (2) A simplified particle-dynamic model was used in the present investigation, which can only predict the mean particle size while these is a particle size distribution in the experiments. (3) In the modeled reaction mechanism, only the oxidation of $TiCl_4$ is considered while the hydrolysis is neglected. The hydrolysis kinetics may have effects on particle sizes. But there is no published hydrolysis kinetics to our knowledge. (4) There is a recirculation zone near the bottom of the diffusion flame but one-dimensional model cannot predict the recirculation. Some generated TiO_2 nanoparticles might stay in that zone for a long time, resulting in much larger particles. Therefore, a comprehensive hydrodynamic model should be used together with the particle-dynamic model [16] have taken the flow field into consideration. (5) In experiments, a ceramic filter placed at the top of the diffusion flame is operated at relatively high temperature (between 100 and 200 °C). The captured titania nanoparticles might be sintered to larger particles.

5. Conclusions

TiO_2 nanoparticles were synthesized using air, $TiCl_4$ and LPG in the diffusion flame. Based on the isothermal assumption, a particle-dynamic model was used to study the nucleation, coagulation and sintering processes during the nanoparticles generation. The following conclusions can be drawn: (1) Under the optimal experimental condition (airflow rate: 61.1 cm^3/s, LPG flow rate: 1.17 cm^3/s), the mean diameter of the synthesized particle is less than 20 nm. (2) The diameter of synthesized nanoparticles increases obviously with the LPG flow rate, and increases slightly with the airflow rate. (3) Most of the product are the anatase. The rutile content increases with the increasing flame temperature. (4) The particle size is affected by the flame height, while the particle size distribution is determined primarily by the flame shape. (5) The results of the particle-dynamic model agree with measured data when the $TiCl_4$ feed concentrations are relatively low. (6) A comprehensive hydrodynamic model, which can describe the complex flow patterns of the diffusion flame, should be used together with the particle-dynamic model to predict size of titania nanoparticles more accurately.

Acknowledgments

The project was supported by the National Natural Science Foundation of China (NNSFC, No. 20476065), the Scientific Research Foundation of State Education Ministry (SRF for ROCS, SEM) and the Key Lab. of Multiphase Reaction of the Chinese Academy of Science (No. 2003–5). The corresponding author would like to thank Prof. S.E. Pratsinis at the Institute of Process Engineering of the Swiss Federal Institute of Technology for sending the offprints of his papers.

References

[1] M.A. Fox, M.T. Dulay, Heterogeneous photocatalysis, Chem. Rev. 93 (1) (1993) 341–347.
[2] G.P. Fotou, S. Vemury, S.E. Pratsinis, Synthesis and evaluation of titania powders for photocatalysis of phenol, Chem. Eng. Sci. 49 (1994) 4939–4948.
[3] G.P. Fotou, S.E. Pratsinis, Photocatalytic destruction of phenol and salicylic acid with aerosol and commercial titania powders, Chem. Eng. Commun. 151 (1996) 251.
[4] F. Ansorge, C. Fusel, Preparation and thermoelectricity of titania/vanadium(V) oxide powders, J. Mater. Sci. 28 (1) (1993) 40–44.
[5] B.C. Liu, J.T. Wang, Studies on the preparation of TiO_2 powders by hydrolysis, J. Nanjing Univ. Chem. Tech. 19 (4) (1997) 76–79 (in Chinese).
[6] J.C. Zhang, W.L. Zeng, Preparation of TiO_2 ultrafine powder in terms of SCFD technique, J. Inorg. Mater. 14 (1) (1999) 29–35 (in Chinese).
[7] D.J. Hee, Effects of H_2O on the particle size in the vapor-phase synthesis of TiO_2, Ceram. Process. 43 (11A) (1997) 2704–2709.
[8] K. Segawa, M. Katsuta, F. Kameda, TiO_2-coated on Al_2O_3 support prepared by the CVD method for HDS catalysis, Catal. Today 29 (1) (1996) 215–219.
[9] G.L. Zheng, B. Ma, J.R. Rong, J.G. Wang, R.Y. Hong, Plasma synthesis of nanometer oxide powders for catalysts, in: Proceedings of the 13th International Symposium on Plasma. Chem., vol. 4, Beijing, 1997, pp. 1684–1689.
[10] M.K. Akhtar, S. Vemury, S.E. Pratsinis, Competition between $TiCl_4$ Hydrolysis and Oxidation and Its Effect on Product TiO_2 Powder, AIChE J. 40 (1994) 1183.
[11] S.E. Pratsinis, W.H. Zhu, S. Vemury, The role of gas mixing in flame synthesis of titania powders, Powder Technol. 86 (1) (1996) 87–93.
[12] T. Johannessen, S.E. Pratsinis, H. Livbjerg, Computational analysis of coagulation and coalescence in the flame synthesis of titania, Powder Technol. 118 (2001) 242–250.
[13] H.K. Kammler, S.E. Pratsinis, P.W. Morrison, B. Hemmerling, Flame temperature measurements during electrically assisted aerosol synthesis of nanoparticles, Combust. Flame 128 (4) (2002) 369–381.
[14] R. Mueller, H.K. Kammler, K. Wegner, S.E. Pratsinis, The OH-surface density of SiO_2 and TiO_2 by thermogravimetric analysis, Langmuir 19 (2003) 160–165.
[15] K-S. Kim, J-K. Kim, W-S. Kim, Influence of reaction conditions on sol-precipitation process producing silicon oxide particles, Ceram. Int. 28 (2002) 187–194.
[16] B.W. Lee, J.I. Jeong, J.Y. Hwang, M. Choi, S.H. Chung, Analysis of growth of non-spherical silica particles in a counterflow diffusion

flame considering chemical reactions, coagulation and coalescence, Aerosol Sci. 32 (2001) 165–185.
[17] J.D. Landgrebe, S.E. Pratsinis, Gas-phase manufacture of particles: interplay of chemical reaction and aerosol coagulation in the free-molecular regime, Ind. Eng. Chem. Res. 28 (1989) 1474–1481.
[18] R.Y. Hong, Z.Q. Ren, H.Z. Li, Thermodynamic and particle-dynamic study for combustion synthesis of titania nanoparticles, China Particuol. 2 (2) (2004) 63–69.
[19] F.E. Kruis, K.A. Kusters, S.E. Pratsinis, B. Scarlett, A simple model for the evolution of the characteristics of aggregate particles undergoing coagluation and sintering, Aerosol Sci. Tech. 19 (1993) 514–526.
[20] A. Schild, A. Gutsch, H. Muhlenweg, S.E. Pratsinis, Simulation of nanoparticle production in premixed aerosol flow reactors by interfacing fluid mechanics and particle dynamics, J. Nanoparticle Res. 1 (1999) 305–315.
[21] S.E. Pratsinis, H. Bai, P. Biswas, M. Frenklach, S.V.R. Mastrangelo, Kinetics of $TiCl_4$ oxidation, J. Am. Ceram. Soc. 73 (1990) 2158–2162.
[22] W. Koch, S.K. Friedlander, The effect of particle coalescence on the surface area of a coagulation aerosol, J. Colloid Interface Sci. 140 (1990) 419–427.
[23] J.H. Seinfeld, Atmospheric Chemistry and Physics of Air Pollution, John Wiley & Sons, New York, 1986.
[24] A. Kobata, K. Kusakabe, S. Morooka, Growth and transformation of TiO_2 crystallites in aerosol reactor, AIChE J. 37 (3) (1991) 347–359.
[25] D.W. Schaefer, A.J. Hurd, Growth and structure of combustion aerosols, Aerosol Sci. Tech. 12 (1990) 876–890.
[26] W.H. Zhu, S.E. Pratsnis, Synthesis of SiO_2 and SnO_2 particles in diffusion flame reactors, AIChE J. 43 (11A) (1997) 2657–2669.
[27] L.Y. Shi, C.D. Li, Study on the nanosized TiO_2 particles synthesized by $TiCl_4$ high temperature gas phase oxidation II. Crystal structure controlling, Funct. Mater. 3l (6) (2000) 625–627 (in Chinese).
[28] R.Y. Hong, Z.H. Shen, Nanosized ZnO prepared by microwave homogeneous precipitation and its photocatalytic property, Chin. J. Proc. Eng. 5 (6) (2005) (in Chinese).
[29] R.Y. Hong, L.P. Xu, Z.Q. Ren, H.Z. Li, Nanosized ZnO prepared by homogeneous precipitation and its photocatalytic property, Chem. Eng. Environ. Prot. 6 (3) (2005) (in Chinese).
[30] J.D. Landgrebe, S.E. Pratsinis, S.V.R. Mastrangelo, Nomographs for vapor synthesis of ceramic powders, Chem. Eng. Sci. 45 (9) (1990) 2931–2941.